Molecular Biology of the Cell
Vol. 18, 2473–2480, July 2007

A Cytosolic Splice Variant of Cab45 Interacts with Munc18b and Impacts on Amylase Secretion by Pancreatic Acini

Patrick P.L. Lam,* Kati Hyvärinen,†‡ Maria Kauppi,† Laura Cosen-Binker,* Saara Laitinen,† Sirkka Keränen,§ Herbert Y. Gaisano,* and Vesa M. Olkkonen†

*Department of Medicine, University of Toronto, Toronto, Ontario, Canada M5S 1A8; †Department of Molecular Medicine, National Public Health Institute, Biomedicum, FI-00251 Helsinki, Finland; ‡Institute of Dentistry, University of Helsinki, FI-00014 Helsinki, Finland; and §Technical Research Center of Finland, FI-02044 VTT, Finland

Submitted October 24, 2006; Revised April 3, 2007; Accepted April 5, 2007
Monitoring Editor: Adam Linstedt

We identified in a yeast two-hybrid screen the EF-hand Ca^{2+}-binding protein Cab45 as an interaction partner of Munc18b. Although the full-length Cab45 resides in Golgi lumen, we characterize a cytosolic splice variant, Cab45b, expressed in pancreatic acini. Cab45b is shown to bind $^{45}Ca^{2+}$, and, of its three EF-hand motifs, EF-hand 2 is demonstrated to be crucial for the ion binding. Cab45b is shown to interact with Munc18b in an in vitro assay, and this interaction is enhanced in the presence of Ca^{2+}. In this assay, Cab45b also binds the Munc18a isoform in a Ca^{2+}-dependent manner. The endogenous Cab45b in rat acini coimmunoprecipitates with Munc18b, syntaxin 2, and syntaxin 3, soluble *N*-ethylmaleimide-sensitive factor attachment protein receptors with key roles in the Ca^{2+}-triggered zymogen secretion. Furthermore, we show that Munc18b bound to syntaxin 3 recruits Cab45b onto the plasma membrane. Importantly, antibodies against Cab45b are shown to inhibit in a specific and dose-dependent manner the Ca^{2+}-induced amylase release from streptolysin-O–permeabilized acini. The present study identifies Cab45b as a novel protein factor involved in the exocytosis of zymogens by pancreatic acini.

INTRODUCTION

The exocrine acinar cells of the pancreas constitute a well established model for the study of regulated exocytosis in nonexcitable polarized cells (for review, see Wäsle and Edwardson, 2002; Williams, 2006). They synthesize a variety of digestive enzymes, which are released into the pancreatic duct and the duodenum upon demand. The enzymes are transported from the *trans*-Golgi network to zymogen granules (ZGs) in the form of inactive proenzymes. The condensing granules undergo a series of maturation steps that involve concentration of the zymogens and reduction of membrane surface. The mature ZGs are found predominantly in the apical region of the cells. Exocytosis of the zymogens occurs via the apical surface of the acinar cells, which accounts for <10% of the cell surface area. The ZGs are clamped from undergoing spontaneous release, and binding of secretagogues such as acetylcholine or cholecystokinin to cell surface receptors activates well characterized Ca^{2+}-dependent signal transduction pathways, evoking rearrangements of the actin cytoskeleton and apical exocytosis (Gaisano, 2000; Wäsle and Edwardson, 2002; Williams, 2006).

It is widely accepted that the core machinery responsible for membrane fusion in intracellular vesicle transport consists of membrane-anchored proteins denoted as soluble *N*-ethylmaleimide-sensitive factor attachment protein receptors (SNAREs) (for review, see Rothman, 2002; Jahn and Scheller, 2006). In ZG exocytosis from acinar cells, the relevant target membrane SNAREs (t-SNAREs) are syntaxin 2 (syn2) reported to reside in the apical membrane, and syntaxin 3 (syn3), which localizes to the ZG limiting membrane (Gaisano *et al*., 1996, 1997). Digestion of syn2 with botulinum toxin C resulted in complete inhibition of ZG–plasma membrane fusion, demonstrating a central role of this t-SNARE in ZG exocytosis (Hansen *et al*., 1999). The major vesicle SNARE (v-SNARE) detected on the ZG is vesicle-associated membrane protein (VAMP)2, but proteolytic cleavage of this protein by tetanus toxin only caused partial inhibition of ZG exocytosis (Gaisano *et al*., 1994). A knockout mouse model suggests VAMP8/endobrevin as a v-SNARE with a key role in ZG exocytosis in acini (Wang *et al*., 2004). Toxin cleavage experiments suggested that syn3 on the granule membranes is involved in homotypic fusion of the granules (Hansen *et al*., 1999), which is an important part for the compound fusion process leading to rapid secretion of large amounts of zymogens upon stimulus (Nemoto *et al*., 2001; Pickett and Edwardson, 2006). Furthermore, the small GTPases Rab3D and Rab27b are present on ZG and regulate zymogen secretion from acini (Ohnishi *et al*., 1997; Chen *et al*., 2002, 2004; Pickett and Edwardson, 2006).

This article was published online ahead of print in *MBC in Press* (http://www.molbiolcell.org/cgi/doi/10.1091/mbc.E06–10–0950) on April 18, 2007.

Address correspondence to: Herbert Gaisano (herbert.gaisano@utoronto.ca) or Vesa Olkkonen (vesa.olkkonen@ktl.fi).

Abbreviations used: GST, glutathione *S*-transferase; SM, Sec1–Munc18 protein; SLO, streptolysin-O; SNARE, soluble *N*-ethylmaleimide-sensitive factor attachment protein receptor; syn, syntaxin; ZG, zymogen granule; wt, wild-type.

The Sec1–Munc18 (SM) proteins are essential accessory components of the SNARE machineries. These cytosolic proteins interact with specific syntaxins, modulating the capacity of these t-SNAREs to interact with their cognate SNARE partners [reviewed in (Gallwitz and Jahn, 2003; Toonen and Verhage, 2003)]. In mammals there are seven SM proteins, of which the Munc18 isoforms a, b, and c are involved in exocytosis at the plasma membrane. Pancreatic acinar cells express Munc18b and c. Munc18b, which interacts with both syn2 and syn3, was found to be present on the acinar cell plasma membrane and on the ZG (Gaisano *et al*., 1999). Munc18c was reported to localize on the basal membrane where it interacts with syn4, and release of this SM protein from the basal surface by supramaximal cholecystokinin stimulation was suggested to redirect apical exocytosis to the basal membrane (Gaisano *et al*., 2001). Munc18b has been shown to control apical exocytosis in several epithelial cell types (Riento *et al*., 2000; Kauppi *et al*., 2002), H^+-ATPase insertion into the apical membrane of kidney inner medullary collecting duct cells (Nicoletta *et al*., 2004), and mast cell granule secretion (Martin-Verdeaux *et al*., 2003). Furthermore, Munc18b was recently shown to impact on amylase release from rat parotid acinar cells by controlling the interaction of the synaptotagmin-like protein Slp4-a/granuphilin with syn2 and -3 (Fukuda *et al*., 2005).

The exact mechanisms by which the ZG fusion is clamped in the absence of stimulus and by which the Ca^{2+} signals are transmitted to the fusion machinery are poorly understood (Wäsle and Edwardson, 2002; Williams, 2006). In the present study, we identify a novel interaction partner of Munc18b in pancreatic acini, a Ca^{2+}-binding EF-hand protein Cab45b, and we provide evidence for its function in the ZG exocytosis process.

MATERIALS AND METHODS

Antibodies and Other Reagents

Antibodies against Cab45b were produced in New Zealand White rabbits, which were immunized with glutathione *S*-transferase (GST)-Cab45b (see below) by using a standard protocol. The antibodies were affinity purified on a CNBr-Sepharose 4B column (GE Healthcare, Little Chalfont, Buckinghamshire, United Kingdom) with coupled GST-Cab45b as described previously (Laitinen *et al*., 2002). The anti-SNAP23 antiserum was generated in a similar manner. The anti-Munc18b antiserum was generated as described previously (Riento *et al*., 1996). The rabbit anti-syn2 and -syn3 as well as mouse monoclonal anti-tubulin were from Sigma-Aldrich (St. Louis, MO), rabbit anti-VAMP2 was from Stressgen (Nventa Biopharmaceuticals, San Diego, CA), and mouse monoclonal anti-Na^+/K^+-ATPase was from Upstate Biotechnology-Chemicon International (Temecula, CA). Rabbit antibody against Munc 18c was a gift from Dr. Y. Tamori (Kobe University, Kobe, Japan). Recombinant streptolysin-O (rSLO) was purchased from S. Bhakdi (University of Mainz, Mainz, Germany).

Yeast Two-Hybrid Screening

The full-length Madin-Darby canine kidney (MDCK)II cell Munc18b cDNA (accession no. L41609) was cloned in the GAL4 DNA binding domain bait vector pGBT9 (Clontech, Mountain View, CA), and transformed into the *Saccharomyces cerevisiae* strain HF7c. Interacting clones were selected from a human lymphocyte cDNA library in the pACT GAL4 activation domain vector (catalog no. HL4006AE; Clontech) by using Leu-Trp-His triple selection according to the manufacturer's instructions. Of the clones surviving the selection, those positive in an 5-bromo-4-chloro-3-indolyl-β-D-galactoside test were included for further analysis. After removal of the bait plasmid in the absence of Trp selection, the prey plasmids were isolated and transformed into *Escherichia coli* DH5α to produce DNA for sequencing.

Identification of Cab45 Splice Variants in the Pancreas

Initially, the National Center for Biotechnology Information sequence database was searched with the human Cab45 sequence (accession no. NM_016176), revealing a number of putative splice variants lacking exon 2, which encodes the cleavable amino-terminal signal sequence of Cab45. Thereafter, oligonucleotide primers ATATGAATTCGAAAGATGGCAGTGGCCTGATC (forward) and ATATGAATTCGCGTCGGCA ACCTCCTTCTC (reverse) annealing with human Cab45 exons 1 and 4, respectively, were designed. These primers were used to amplify and clone sequences from human pancreatic cDNA. The clones in pBluescript SK(−) (Stratagene, LaJolla, CA) were sequenced with a cycle-sequencing kit (BigDye; Applied Biosystems, Foster City, CA) and an automated ABI3730 sequencer (Applied Biosystems). This revealed cDNAs that are spliced directly from exon 1 to exon 4. To further verify the existence of such variants (denoted as b-variants) in the pancreas, a 5′ primer, GGCAGACCGGACGAGTATAAG, with nine bases from exon 1 and 12 bases from exon 4, and a 3′ primer, GGTGGGGTCCGGGACAGCC, from exon 7 (downstream of the stop codon) were used to selectively amplify b-variants from cDNAs transcribed from human total mRNAs from colon, heart, kidney, liver, lung, pancreas, and skeletal muscle (Stratagene). The reverse transcription was carried out using the above-mentioned primer that anneals with Cab45 exon 7 and the Pfu Turbo polymerase (Stratagene). To produce a cDNA for the Cab45b splice variant, the cDNA fragment encoding amino acid region M262-F362 of Cab45 was isolated by polymerase chain reaction (PCR) by using the full-length Cab45a cDNA as template and the primers ATATGGATCCATGCTCAGGTTCATGGTGAAGG and TCCGGAATTCTCAAAACTCCTCGTGCACGC. From here on, the amino acid (aa) residues of Cab45b are numbered M1-F130.

Production of Wild-Type (wt) and Mutant Cab45b Proteins in E. coli

For protein production in *E. coli*, the Cab45b cDNA was subcloned into the BamHI/EcoRI sites of pGEX1λT (GE Healthcare). For production of site-specifically mutated protein variants, mutagenesis was carried out on Cab45b-pGEX1λT by using the Quikchange kit (Stratagene). Point mutations were generated in EF-hand 1 (E25Q), EF-hand 2 (E70Q), and EF-hand 3 (E106Q). In addition, all three combinations of two EF-hand mutations were created. N- or C-terminally truncated variants making up aa residues D41-F130 and M1-G116, respectively, were generated by PCR, and the cDNA fragments obtained were inserted in the same vector. All constructs were verified by sequencing using a cycle sequencing kit (BigDye) and an automated ABI3730 sequencer (Applied Biosystems). The GST fusion proteins were produced in *E. coli* strain BL21(DE3) and purified on glutathione-Sepharose 4B (GE Healthcare) according to the manufacturer's instructions. Protein concentrations were determined by using the DC assay (Bio-Rad, Hercules, CA).

Production of His_6-tagged Munc18b in Insect Cells

A recombinant baculovirus expressing His_6-Munc18b was generated and used for protein production in Sf9 cells as described previously (Riento *et al*., 2000). The protein was purified on nickel-nitrilotriacetic acid agarose (QIAGEN, Valencia, CA) according to the manufacturer's instructions.

Western Blotting

For visualization of Cab45b, rat pancreas snap frozen in liquid N_2 was thawed and homogenized directly in Laemmli sample buffer containing the complete protease inhibitor cocktail (Roche Diagnostics, Mannheim, Germany), followed by incubation in a boiling water bath for 5 min. Approximately 20 μg of total protein (estimated from Coomassie-stained gels) was applied in 15% SDS-polyacrylamide gel electrophoresis (PAGE) gels, and the separated proteins were transferred onto Hybond-C Extra nitrocellulose filter (GE Healthcare). The filters were incubated with anti-Cab45b antiserum, and the bound antibodies visualized using goat anti-rabbit IgG (H+L) horseradish peroxidase conjugate (Bio-Rad) and enhanced chemiluminescence (ECL; GE Healthcare) followed by visualization by exposure to Kodak X-OMAT AR films (Eastman Kodak, Rochester, NY). For inhibition of specific Cab45b immunoreactivity, 200 μg/ml purified GST-Cab45b (see above) was incubated for 3 h at room temperature with the primary antibody, before the antibody was applied on the filter.

Immunoprecipitation

Lysates of rat acini containing equal amounts of protein were clarified by centrifugation (12,000 × *g*; 10 min). Aliquots of the resulting supernatants containing 600 μg of protein, precleared for 40 min by using 40 μl of 50% suspension of protein G-Sepharose (GE Healthcare), were incubated with Munc18b or Cab45b antibodies. Immunocomplexes were captured using 40 μl of protein G-Sepharose, which was washed four times with lysis buffer containing 1 mM Na_3VO_4. Samples of immunoprecipitated proteins or total cell lysates were dissolved in Laemmli buffer and boiled for 5 min. Equal amounts of protein were separated on 8% SDS-PAGE and transferred to nitrocellulose membranes (Bio-Rad), which were blocked for 1 h in Tris-buffered saline containing 5% bovine serum albumin (BSA) and then incubated with the appropriate primary antibodies. The bound antibodies were visualized using relevant peroxidase-coupled secondary antibodies and ECL.

Calcium Binding Assay

Plain GST and the purified GST-Cab45b (wild-type and all mutant/truncated proteins), 0.5 μg each, were resolved on 12.5% SDS-PAGE, electrotransferred

onto Hybond-C extra nitrocellulose filter (GE Healthcare), and allowed to renature for 1 h in 60 mM KCl, 10 mM imidazole, 5 mM $MgCl_2$, pH 6.8. The filters were probed for 10 min at room temperature with $^{45}Ca^{2+}$ (11.63 mCi/mg; PerkinElmer, Wellesley, MA), at 1 μCi/ml in the above-mentioned buffer, washed with H_2O, and exposed on Kodak X-OMAT AR films.

In Vitro Assay for Munc18–Cab45b Interaction

MaxiSorb 96-well plates (NUNC A/S, Roskilde, Denmark) were coated with GST-Cab45b (3 μg/well) in 50 mM $NaHCO_3$ buffer, pH 9.6, for 16 h at 4°C. The binding of [^{35}S]methionine-labeled in vitro transcribed/translated (Tnt-coupled rabbit reticulocyte system; Promega, Madison, WI) Munc18a, Munc18b, Munc18b to the immobilized GST-Cab45b was assayed essentially as described in Riento *et al*. (2000), with the exceptions that unspecific binding was now blocked with 1% BSA, 0.05% Tween 20 in 10 mM HEPES, pH 7.2, and incubation of the in vitro-translated radioactive Munc18 proteins was carried out overnight at 4°C. Ten micromolar $CaCl_2$ or 100 μM EGTA was added to the in vitro-translated Munc18b and to the washing buffer. For the Munc18b binding curve, 2500–250,000 cpm of the in vitro translation mixture was used. When the interactions of Munc18b, Munc18a, and Munc18c proteins were compared, equal amounts of radioactivity (100,000 cpm) were used. The numbers of methionine residues in the three proteins are rat Munc18a, 19; canine Munc18b, 15; and mouse Munc18c, 16. Background binding to wells coated with plain GST was measured in all experiments. For competition of Munc18b binding to Cab45b, 0, 1, 3, or 10 μg of His_6-Munc18b purified from insect cells was added in the in vitro-translated Munc18b aliquots (25,000 cpm) before addition in the GST-Cab45b–coated wells.

Transfection and Immunofluorescence Microscopy

The Cab45b cDNA subcloned into the mammalian expression vector pcDNA4HisMaxC (Invitrogen, Carlsbad, CA) was transfected into the Chinese hamster ovary (CHO)-K1 cell line alone or together with MDCKII Munc18b/pcDNA3.1 (Invitrogen) and/or rat syn3/pBK-CMV (Stratagene) expression plasmids, using Lipofectamine 2000 reagent (Invitrogen). After 24 h, the cells were fixed with 4% paraformaldehyde, 250 mM HEPES, pH 7.4, permeabilized with 0.05% Triton X-100/phosphate-buffered saline, and processed for indirect immunofluorescence microscopy as described previously (Johansson *et al*., 2005). The bound primary antibodies were visualized using anti-mouse and anti-rabbit immunoglobulin G (IgG)-Alexa488 and -568 conjugates (Invitrogen), and the specimens were observed/images recorded with a TCS SP1 laser scanning confocal microscope (Leica, Heidelberg, Germany). Shift of the expressed Cab45b to the plasma membrane was quantified blind by visual judgment from three independent coverslips. From each double- or triple-transfected coverslip, 100 or 50 transfected cells, respectively, were analyzed.

Assay for Amylase Release from SLO-permeabilized Acini

Rat acini were prepared by collagenase digestion as described previously (Gaisano *et al*., 2001). Isolated acini were suspended at 4°C in a permeabilization buffer consisting of 20 mM piperazine-*N*,*N*′-bis-2-ethanesulfonic acid, pH 6.6, 139 mM K^+-glutamate, 4 mM EGTA, 1.78 mM $MgCl_2$, 2 mM MgATP, 0.1 mg/ml soybean trypsin inhibitor, 1 mg/ml bovine serum albumin, and 1 μg/ml rSLO and divided into 200-μl aliquots. rSLO does not require reducing because the single thiol group of wild-type SLO has been removed (Pinkney *et al*., 1989). We have evaluated that this concentration of rSLO under the present incubation conditions induces 90–100% permeabilization as determined using trypan blue staining. Acini in rSLO-containing buffer were incubated in 4°C for a minimum of 10 min to allow toxin to partition into the plasma membrane. Excess rSLO in the supernatant was removed by low-speed centrifugation, and the pellet was resuspended in fresh permeabilization buffer at 200 μl/cell aliquot. The acini were then incubated at 37°C for 3 min to initiate pore formation. For experiments on antibody inhibition of amylase release, nonimmune rabbit IgG, total IgG from a rabbit immunized with Cab45b, or affinity-purified anti-Cab45b antibodies were added to rSLO-permeabilized acini at a final concentration of 0, 0.1, 1.0, 10, 40, or 100 μg/ml and incubated at 37°C for 30–45 min. Ca^{2+}-evoked amylase secretion was then induced with an equal volume of ice-cold permeabilization buffer supplemented with $CaCl_2$ at either low (0.05 mM $CaCl_2$ = 10 nM free Ca^{2+}) or high (9.8 mM $CaCl_2$ = 10 μM free Ca^{2+}) concentration to reach the desired free Ca^{2+} level that was calculated as described previously (Kitagawa *et al*., 1990). Amylase released into the supernatant during the incubation was quantified using a colorimetric method described previously and expressed as a percentage of total cellular amylase (Gaisano *et al*., 2001). Total amylase is the sum of the amylase in the supernatant and acinar cell pellet, from which the stimulated amylase is expressed as a percentage of total amylase. To obtain the net stimulated release, mean basal release (10 nM Ca^{2+}) performed in every experiment was subtracted from mean stimulatory release (10 μM Ca^{2+}).

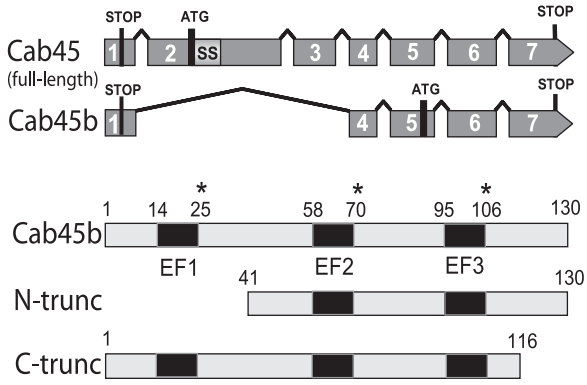

Figure 1. Structures of the human Cab45b mRNA and protein. (A) The mRNAs encoding full-length Cab45 (Cab45a) or Cab45b. The exons are numbered 1–7; ATG, methionine start codon; STOP, stop codon; SS, cleavable amino-terminal signal sequence of Cab45a. The genomic structure was elucidated by blasting the Cab45a cDNA sequence (NM_016176) against the human genome at National Center for Biotechnology Information. (B) Schematic presentation of Cab45b structure. The numbers indicate amino acid positions; EF-hands 1, -2, and -3 are shown. Point mutations in the EF hands are indicated with and asterisk (*). N-trunc and C-trunc represent the N- and C-terminally truncated protein variants, respectively.

RESULTS

Identification of a Novel Interaction Partner of Munc18b

Syntaxins are so far the only known binding partners for Munc18b, whereas its neuronal counterpart Munc18a binds several other protein factors involved in regulated secretion (Toonen and Verhage, 2003). To identify novel interaction partners for Munc18b, we carried out a yeast two-hybrid screen of a human lymphocyte cDNA library. This yielded 74 cDNAs, 68 of which represented sequences that encode Cab45, a previously identified Ca^{2+}-binding protein with six EF-hand motifs (Scherer *et al*., 1996; Koivu *et al*., 1997; Honore and Vorum, 2000). The longest cDNAs represented the full-length coding region, and the shortest cDNA a fragment of amino acids Q269-F362 that contains two EF-hand motifs. Cab45 carries a cleavable signal sequence and has been characterized as a soluble protein that localizes to the Golgi lumen (Scherer *et al*., 1996; Koivu *et al*., 1997).

Because Munc18b is cytosolic, a genuine interaction with Cab45 was initially regarded as unlikely. However, search of sequence databases with the full-length human Cab45 sequence revealed a number of expressed sequence tags from different sources that lacked exon 2 encoding the amino-terminal signal sequence (e.g., AL546806 from human placenta and AL558725 from human T cells). Because such mRNAs may encode cytosolic variants of Cab45, we sought for such mRNAs in the human pancreas by shotgun cloning reverse transcriptase (RT)-PCR products amplified using primers that anneal with exons 1 and 4 of Cab45 (Figure 1A), and the cDNA fragments obtained were sequenced. Of the 12 fragments sequenced, six represented variants that skipped exon 2, the splice acceptor site located at the junction of exons 1 and 2 and the donor sites in the junction of exons 3 and 4 or within exons 2 or -3. To further verify the existence of such splice variants, we designed a forward primer whose 5′ half anneals with exon 1 and whose 3′ half anneals with exon 4. This "exon1/4 primer" was used for RT-PCR from mRNA of different human tissues, together with a primer from downstream of the Cab45 stop codon in exon 7. The primer pair did not amplify anything from a

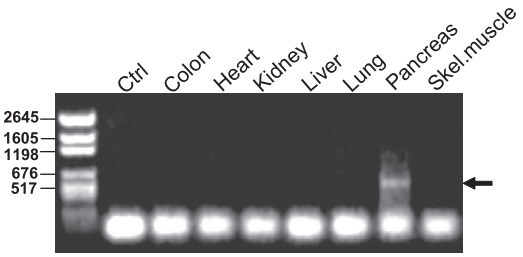

Figure 2. Reverse transcriptase-PCR assay for Cab45b mRNA in human tissues. Total RNA from the indicated human tissues was reverse transcribed as specified in *Materials and Methods*, and the resulting cDNA was amplified with primers specific for the Cab45b splice variant. Mobilities of size markers (base pairs) are indicated on the left. Ctrl, water control (no RNA in reverse transcriptase reaction). The specific 510-base pair product is indicated with an arrow.

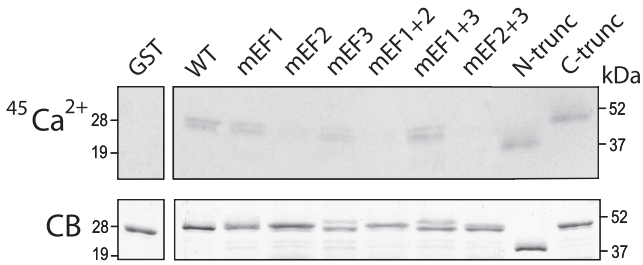

Figure 4. Calcium binding is inhibited by inactivation of Cab45b EF-hand 2. Equal amounts of GST-fusion proteins of wt Cab45b, mutants with one or two EF-hands inactivated (mEF1, mEF2, and so on), and the N- or C-terminally truncated proteins (N-trunc and C-trunc, respectively) were resolved on SDS-PAGE and transferred to nitrocellulose, followed by probing with $^{45}Ca^{2+}$ (top). A Coomassie-stained gel (CB) of the specimens showing equal loading is displayed in the bottom panel. Plain GST (GST) was included as a negative control. Mobilities of molecular mass markers are indicated.

plasmid template carrying the full-length Cab45a cDNA, demonstrating specificity for the desired type of splice variant (data not shown). The tissue RT-PCR analysis revealed a product of the expected size (510 base pairs) in the pancreas. In the other tissues, hardly any products were detectable (Figure 2). Further RT-PCR analysis using 3′ primers from exons 4 and -5 confirmed that the splice variant, denoted from hereon as Cab45b, is in its 3′ parts similar to full-length Cab45 (data not shown). Skipping of exons 2 and -3 in Cab45b results in a protein that is initiated at M232 of the full-length reading frame and consists of 130 amino acid residues and three EF-hand motifs (D14-E25, D58-E70, and D95-E106) predicted by the SMART software (http://smart.embl-heidelberg.de/) (Figure 1B). The deduced molecular mass of the protein is 15,139 kDa.

Cab45b Protein Is Present in Rat Pancreatic Acini

To study the presence of such a short Cab45 variant protein in rat pancreas, we created rabbit antibodies against GST-Cab45b produced in *E. coli*. Western blotting using the antiserum detected in a total protein preparation of rat acini a major protein with the apparent molecular mass of 13 kDa and a weaker reactive band with an apparent mass of 44 kDa (Figure 3A). The size of the 13-kDa protein is consistent with the deduced mass of Cab45b, 15.1 kDa, and that of the larger protein with the deduced mass of the full-length Cab45 isoform, 41.8 kDa. Preincubation of the antibody with purified GST-Cab45b at 200 μg/ml specifically abolished both reactivities, demonstrating that the proteins indeed represent the endogenous Cab45 isoforms in the pancreas. The presence of the strongly reactive 13-kDa band further supports the notion that a short cytosolic variant of Cab45, similar to the Cab45b identified above at the nucleic acid level, is expressed in the pancreas. On immunofluorescence microscopy, the antibody stained in several cell lines the juxtanuclear Golgi apparatus, consistent with the previously reported localization of the endogenous full-length Cab45 isoform (Scherer *et al*., 1996; shown for COS-1 cells in Figure 3B). When Cab45b was expressed in COS-1 cells, it displayed a relatively even cytoplasmic distribution consisting in part of small dots. Some immunostaining was also detected within the nucleus (Figure 3B).

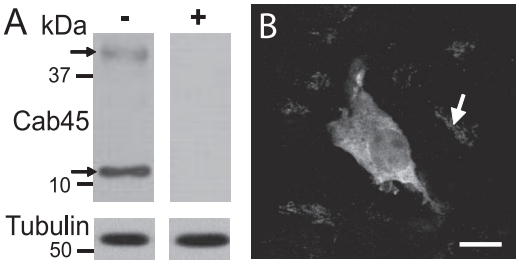

Figure 3. Antibody detection of Cab45b in rat pancreas and COS-1 cells. (A) Total rat pancreas protein extract was Western blotted with anti-Cab45b antiserum (−), or the same antibody preincubated with GST-Cab45b at 200 μg/ml (+). The specific immunoreactive bands of 13 and 44 kDa are indicated with arrows. Mobilities of molecular mass markers are indicated on the left. (B) Immunofluorescence microscopic localization of Cab45 in untransfected COS-1 cells or cells transfected with Cab45b. The transfected cell in the center shows staining of punctate structures within the cytoplasm, whereas the endogenous full-length Cab45 in the surrounding untransfected cells localizes to the juxtanuclear Golgi complex (arrow). Bar, 10 μm.

Cab45b Binds Ca^{2+} Ions, EF-Hand 2 Being Essential for This Activity

To confirm that Cab45b binds Ca^{2+} ions and to investigate the structural requirements for the Ca^{2+} binding, nitrocellulose filter overlay assays with $^{45}Ca^{2+}$ were carried out using wild-type and mutant GST-Cab45b fusion proteins. We generated point mutants with EF-hand 1 (E25Q, denoted mEF1), 2 (E70Q, denoted mEF2), or 3 (E106Q, denoted mEF3) inactivated, and all three combinations of two mutations. In addition, we generated N- and C-terminally truncated constructs making up aa D41-F130 and M1-G116, respectively (Figure 1B). The N-terminal truncation removes EF-hand 1 and part of the region between EF-hands 1 and -2, and the C-terminal truncation 14 aa from the C-terminal end. The overlay assay verified that wt Cab45b binds calcium ions and revealed defective binding by all mutants with EF-hand 2 inactivated, whereas inactivation of EF-hands 1 or -3, or the truncations, did not significantly affect the Ca^{2+} binding (Figure 4).

Interaction of Cab45b and Munc18b In Vitro

To verify in vitro the interaction of Cab45b and Munc18b observed in the two-hybrid system, a previously established solid phase binding assay was used. Here, purified GST-Cab45b was immobilized on Nunc Maxisorb 96-well plates, and association of in vitro-translated [^{35}S]Met-labeled

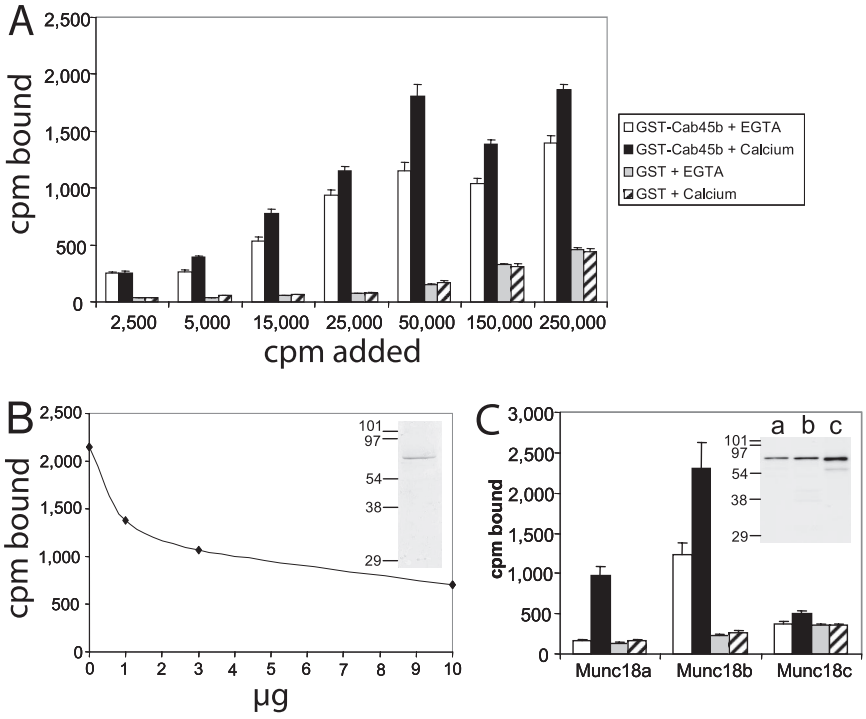

Figure 5. Interaction of Munc18 proteins with Cab45b in vitro. (A) Increasing amounts of in vitro-translated [^{35}S]Met-labeled Munc18b (*x*-axis) were incubated in wells coated with GST or GST-Cab45b. The assay was carried out in the presence or 100 μM EGTA or 10 μM $CaCl_2$. The bound radioactivity (*y*-axis) was quantified by scintillation counting. (B) An assay similar to that described in A was carried out using 25,000 cpm of [^{35}S]Met-labeled Munc18b in the presence of 0, 1, 3, or 10 μg/well (indicated at the bottom) of competing purified His_6-Munc18b. Inset, SDS-PAGE of the His_6-Munc18b used, Coomassie blue staining. Mobilities of molecular mass markers are indicated on the left. (C) Interaction of Munc18a, -b, and -c with Cab45b in the presence or 100 μM EGTA or 10 μM $CaCl_2$. For each Munc18 protein, 100,000 cpm of radioactivity was used. The results are expressed as cpm bound (mean ± SEM; n = 3). The symbols are as in A. Inset, fluorogram of an SDS-PAGE gel showing the [^{35}S]Met-labeled Munc18a, -b, and -c in vitro translation products used. Mobilities of molecular mass markers are indicated on the left.

Munc18b or the related proteins Munc18a and Munc18c with the immobilized Cab45b was assayed as described previously (Riento *et al.*, 2000). Because Cab45b was shown to bind Ca^{2+} ions (see above), binding assays were performed both in the presence and the absence of 10 μM $CaCl_2$. Munc18b was found to associate with Cab45b in a dose-dependent and saturable manner. The background binding to GST represented 7–14% of the signals obtained with GST-Cab45b coating at the amounts of added radioactivity of up to 50,000 cpm. Furthermore, the specific binding of Munc18b to Cab45b was enhanced by an average of 45% in the presence of 10 μM Ca^{2+} (Figure 5A). The specific nature of the interaction detected by using the solid-phase binding assay was verified by competing the binding signal with increasing amounts of purified His_6-Munc18b. The degree of inhibition reached with 10 μg of purified His_6-Munc18b/well was 68% (Figure 5B). In addition to Munc18b, Munc18a was also found to interact with Cab45b. In this case, the binding was abolished in the presence of EGTA, suggesting strong Ca^{2+} dependency. However, Cab45b binding by Munc18c was hardly detectable (Figure 5C).

Immunoprecipitation Confirms the Association of Cab45b and Munc18b in Acini

To analyze the interaction of Munc18b and Cab45b in rat acinar cells, lysates of acini were subjected to immunoprecipitation with either anti-Munc18b or anti-Cab45b antisera, followed by Western blotting of the precipitates by using antibodies against Munc18b, Cab45b, syn2, syn3, synaptosome-associated protein of 23 kDa (SNAP23), VAMP2, Munc18c, tubulin, and Na^+/K^+-ATPase. The results revealed reciprocal and specific coprecipitation of Munc18b and Cab45b (Figure 6). Importantly, both syn2 and syn3, previously known interaction partners of Munc18b, were present in the immunoprecipitates obtained using anti-Munc18b (Figure 6A), and syn3 was also present in the anti-Cab45b immunoprecipitates (Figure 6B). In accordance

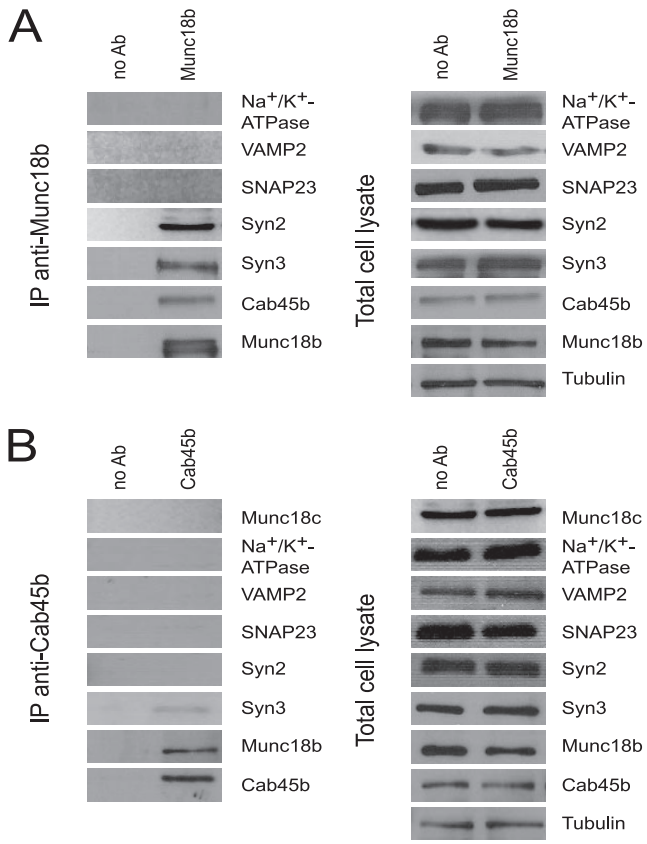

Figure 6. Coimmunoprecipitation of Munc18b and Cab45b from rat acini. Acini lysates were subjected to immunoprecipitation with anti-Munc18b (A) or anti-Cab45b (B) and Western blotted with the antibodies indicated. The immunoprecipitate lanes each represent the precipitate from 600 μg of acinar lysate total protein. Western blots of 15 μg of protein from the total lysates used are shown in the right-hand panels. No Ab, control specimens treated with protein G-Sepharose in the absence of primary antibody.

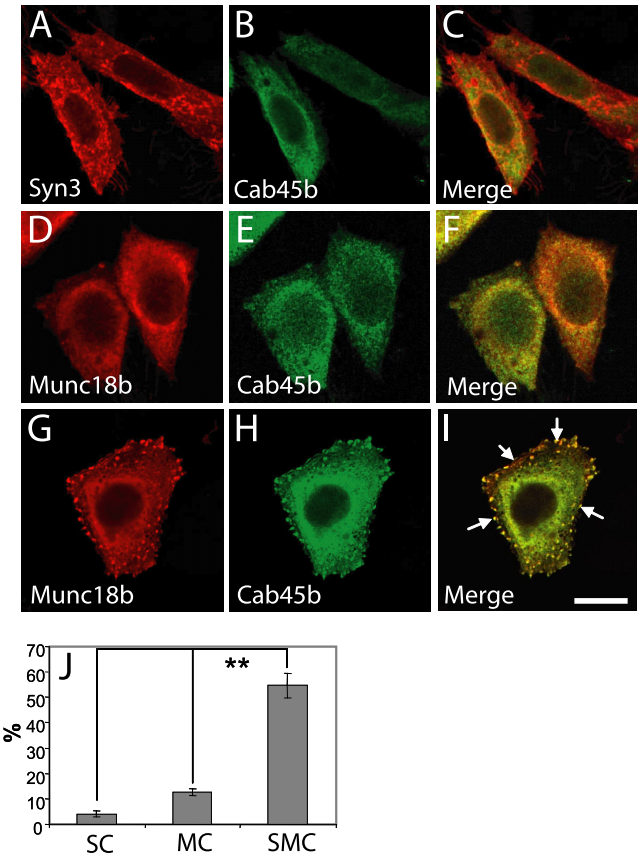

Figure 7. Munc18b is able to recruit Cab45b to the plasma membrane. CHO-K1 cells were transfected for 24 h with expression plasmids encoding and syn3 and Cab45b (tagged with Xpress epitope) (A–C), Munc18b and Cab45b (D–F), or syn3, Munc18b and Cab45b (G–I), and processed for confocal immunofluorescence microscopy. Staining for syn3 (A) and staining for Munc18b (D and G), as detected with specific rabbit antibodies. B, E, and H represent Cab45b visualized with the Xpress antibody. Overlays are shown in C, F, and I. The arrows indicate colocalization of Cab45b with Munc18b at plasma membrane structures. Bar, 10 μm. Quantification of the proportion of cells displaying plasma membrane recruitment of Cab45b is shown in H. The data represent mean ± SEM, n = 3 (**p < 0.01; Student's *t* test). SC, syn3 + Cab45b transfection; MC, Munc18b + Cab45b transfection; SMC, syn3 + Munc18b + Cab45b transfection.

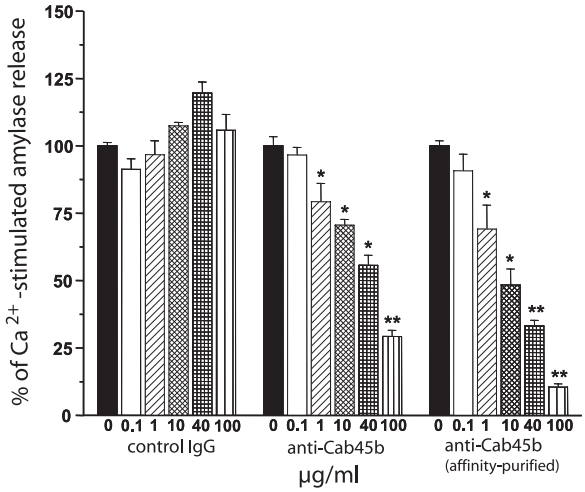

Figure 8. Anti-Cab45b antibodies inhibit Ca^{2+}-evoked amylase release from SLO-permeabilized pancreatic acini. Rat pancreatic acini were permeabilized with SLO and then preincubated with increasing concentrations (identified at the bottom) of control IgG, total IgG from a rabbit immunized with Cab45b (anti-Cab45b), or affinity-purified anti-Cab45b antibodies (anti-Cab45b, affinity-purified), and then they were stimulated with 10 μM Ca^{2+}. Amylase released into the supernatant was determined and expressed as a percentage of mean net amylase release without antibody. The data represents mean ± SEM from five independent experiments each performed in triplicate (*p < 0.05, **p < 0.01; Student's *t* test; difference between treatment with anti-Cab45b and the same concentration of control IgG).

with the observation that Munc18b inhibits the interactions of syntaxins with SNAP23 and v-SNAREs (Riento *et al.*, 1998, 2000), neither SNAP23 nor VAMP2 coprecipitated with Munc18b or Cab45b. The results thus suggested that Cab45b, Munc18b, and at least syntaxin 3 can form a ternary complex. Munc18c, also present in the acini (Gaisano *et al.*, 1999, 2001), was not found in the anti-Cab45b precipitates. The Na^+/K^+-ATPase included as a negative control was not found in the precipitates, further illustrating the specificity of the coimmunoprecipitation observed.

Morphological Evidence for Cab45b–Munc18b Interaction

To further confirm the interaction of Cab45b with Munc18b in live cells, CHO-K1 cells, which do not express detectable amounts of endogenous Munc18b, were transfected with a Cab45b expression construct together with syntaxin 3, Munc18b, or both. In cells double transfected with Cab45b and syn3, the syntaxin was found at the plasma membrane (PM), whereas Cab45b remained distributed as punctate structures in the cytoplasm that only rarely coincided with the PM. In some cells, the protein also showed a tendency to accumulate within the nucleus (Figure 7, A–C). When Cab45b was coexpressed with Munc18b, a similar punctate Cab45b pattern was observed, whereas Munc18b showed an even cytosolic-looking distribution (Figure 7, D–F). However, in specimens triple transfected with Cab45b, syn3, and Munc18b, Munc18b displayed in many cells prominent localization on PM profiles and cell surface blebs, due to interaction with the overexpressed syntaxin 3 (also see Riento *et al.*, 1996). Importantly, pronounced membrane recruitment of Cab45b and a high degree of colocalization with Munc18b were detectable in these cells (Figure 7, G–I). Quantification of the immunofluorescence data confirmed a significant recruitment of Cab45b to the plasma membrane in the cells in which Munc18b was found at PM location (Figure 7H). This finding supports the immunoprecipitation results, suggesting that the shift in Cab45b localization in the triple-transfected cells is due to bridging of Cab45b and syn3 by Munc18b.

Cab45b Antibodies Inhibit Amylase Secretion from SLO-permeabilized Acini

To address the putative function of Cab45b in ZG exocytosis, we carried out amylase secretion assays in acini preparations permeabilized with streptolysin-O. Assays were performed in the presence of nonimmune rabbit IgG, total IgG from a rabbit immunized with Cab45b, or affinity-purified antibodies against Cab45b, by using basal (10 nM) or stimulating (10 μM) Ca^{2+} concentrations. Basal amylase release was similar in control IgG (2.7 ± 0.1% of total cellular amylase) and anti-Cab45b treated acini (which was 3.6 ± 0.4% of total cellular amylase). Release stimulated by 10 μM

Ca^{2+} in the absence of antibodies was typically ~24 ± 0.7% of total amylase before subtraction of the basal levels. Addition of pre-immune rabbit IgG in the permeabilized acini at concentrations up to 100 μg/ml did not significantly affect the stimulated release of amylase, whereas both the total and affinity-purified anti-Cab45b IgG preparations induced a dose-dependent and statistically significant inhibition of amylase secretion at concentrations from 1.0 to 100 μg/ml (Figure 8). The affinity-purified anti-Cab45b antiserum displayed a stronger inhibitory effect than the total IgG, the difference between the two preparations being statistically significant ($p < 0.05$) at the 10, 40, and 100 μg/ml concentrations. This observation further supports the specific nature of the inhibition observed.

DISCUSSION

A number of non-syntaxin interaction partners have been identified for the neuronal SM protein Munc18a (Rizo and Südhof, 2002; Gallwitz and Jahn, 2003; Kauppi *et al*., 2004). In the present study, we identified a cytosolic splice variant of the EF-hand calcium-binding protein Cab45 (Scherer *et al*., 1996), as the first non-syntaxin binding partner of Munc18b. The variant, denoted as Cab45b, is expressed in the pancreas, as evidenced by sequencing of shotgun-cloned cDNAs, by RT-PCR with specific primers, and by Western blotting. Cab45b expressed in COS or CHO-K1 cells was shown to have a punctate cytoplasmic localization, suggesting that it associates with yet unidentified cytoplasmic vesicles. The interaction of Munc18b and Cab45b was verified by a solid-phase binding assay using GST-Cab45b and in vitro-translated radioactive Munc18b, and by two-way coimmunoprecipitation from rat acini. The in vitro binding assay and the coimmunoprecipitation study leave open the possibility that the interaction of Munc18b and Cab45b could be indirect. Due to severe problems in handling purified Munc18b, we have been unable to show a direct interaction using pure recombinant proteins. However, identification of Cab45b as a binding partner of Munc18b by the yeast two-hybrid system suggests that the interaction could be direct. Results of the solid-phase binding assay suggest that the interaction between Munc18b and Cab45b is enhanced in the presence of Ca^{2+}. Cab45b was also found to interact with the neuronal SM protein Munc18a, and this interaction showed more pronounced Ca^{2+} dependency than that with Munc18b. Binding of Cab45b by Munc18c, which is present abundantly in acini (Gaisano *et al*., 1999, 2001), was hardly detectable, and the protein was not found in the anti-Cab45b immunoprecipitates. This suggests that Cab45b mainly interacts with Munc18b in the acini.

Our biochemical and morphological results suggest that Munc18b, Cab45b, and at least syn3 are present in a ternary complex; in other words, that Munc18b is able to bind Cab45b and syntaxins simultaneously. That SNAP23 or VAMP2 was absent from the immunoprecipitated Munc18b/Cab45b/syn complexes is consistent with the view that, similar to its neuronal counterpart Munc18a (Misura *et al*., 2000), Munc18b binds the closed conformation of syntaxins (Kauppi *et al*., 2002), and when present in excess amounts, it inhibits the association of syntaxins with SNAP23 or v-SNAREs (Riento *et al*., 1998, 2000). In accordance with this notion, we have recently shown that overexpression of Munc18b in acini inhibits ZG exocytosis (Lam, Kauppi, Huang, Olkkonen, and Gaisano, unpublished data).

Importantly, secretion assays using rSLO-permeabilized acini demonstrated specific and dose-dependent inhibition of Ca^{2+}-induced amylase release by rabbit antibodies against the endogenous Cab45b. This finding strongly supports the notion that Cab45b indeed forms part of the machinery responsible for ZG exocytosis. The exact mode of action of the SM proteins is under debate (Gallwitz and Jahn, 2003; Toonen and Verhage, 2003; Kauppi *et al*., 2004). Several family members are suggested to act as linkers between the Rab GTPase-based machinery for vesicle tethering (Guo *et al*., 2000; Whyte and Munro, 2002) and the SNAREs responsible for fusion (Jahn and Südhof, 1999; Rothman, 2002). Examples of such bridging factors are granuphilin, which binds both Rab3 and Munc18a (Coppola *et al*., 2002); rabenosyn 5, which binds both Rab5 and the SM protein VPS45 (Nielsen *et al*., 2000); and *S. cerevisiae* Vac1p, which binds the GTPase Vps21p and the SM protein Vps45p (Peterson *et al*., 1999; Tall *et al*., 1999). These findings may explain, e.g., the observed role of Munc18a in the docking of large dense core vesicles (Voets *et al*., 2001). Conversely, functions directly associated with the trans-SNARE complex formation and even with fusion pore regulation have been suggested (Misura *et al*., 2000; Fisher *et al*., 2001; Graham *et al*., 2004). Calcium ions play a key role in all regulated secretory events. Therefore, the observed enhancement of the Munc18b–Cab45b interaction in the presence of Ca^{2+} may be highly important. The mechanisms by which the ZG fusion is clamped in the absence of stimulus and by which the signals from Ca^{2+} oscillations are transmitted to the fusion machinery, are poorly understood (Wäsle and Edwardson, 2002; Williams, 2006). Cab45b binds Ca^{2+} and plays a role in zymogen secretion induced by Ca^{2+}. It is therefore a tempting possibility that Cab45b could be involved in the calcium triggering of ZG exocytosis.

ACKNOWLEDGMENTS

We are grateful to Seija Puomilahti and Pirjo Ranta for skilled technical assistance. Prof. Ilkka Julkunen (KTL, Helsinki, Finland) is acknowledged for kind help with protein production in insect cells. This study was supported by Instrumentariumin Tiedesäätiö (M.K.), Farmoksen Tutkimus-ja Tiedesäätiö (M.K.), the Academy of Finland (grants 54301, 206298, 113013, and 118720 to V.M.O.), the Finnish Cultural Foundation (M.K. and V.M.O.), National Institutes of Health (R21-AA015579-01A1, to H.Y.G.), Canadian Diabetes Association (GA-2-06-2115-HG, to H.Y.G.), and the Sigrid Juselius Foundation (V.M.O.). P.P.L.L. is funded by graduate doctoral studentships from the Canadian Digestive Health Foundation and Canadian Institute of Health Research (JDD 77848), the University of Toronto-BBDC Tamarack Award, and the Ontario Graduate Studentship Award.

REFERENCES

Chen, X., Edwards, J. A., Logsdon, C. D., Ernst, S. A., and Williams, J. A. (2002). Dominant negative Rab3D inhibits amylase release from mouse pancreatic acini. J. Biol. Chem. *277*, 18002–18009.

Chen, X., Li, C., Izumi, T., Ernst, S. A., Andrews, P. C., and Williams, J. A. (2004). Rab27b localizes to zymogen granules and regulates pancreatic acinar exocytosis. Biochem. Biophys. Res. Commun. *323*, 1157–1162.

Coppola, T., Frantz, C., Perret-Menoud, V., Gattesco, S., Hirling, H., and Regazzi, R. (2002). Pancreatic beta-cell protein granuphilin binds Rab3 and Munc-18 and controls exocytosis. Mol. Biol. Cell *13*, 1906–1915.

Fisher, R. J., Pevsner, J., and Burgoyne, R. D. (2001). Control of fusion pore dynamics during exocytosis by Munc18. Science *291*, 875–878.

Fukuda, M., Imai, A., Nashida, T., and Shimomura, H. (2005). Slp4-a/granuphilin-a interacts with syntaxin-2/3 in a Munc18-2-dependent manner. J. Biol. Chem. *280*, 39175–39184.

Gaisano, H. Y. (2000). A hypothesis: SNARE-ing the mechanisms of regulated exocytosis and pathologic membrane fusions in the pancreatic acinar cell. Pancreas *20*, 217–226.

Gaisano, H. Y., Huang, X., Sheu, L., Ghai, M., Newgard, C. B., Trinh, K. Y., and Trimble, W. S. (1999). Snare protein expression and adenoviral transfection of amphicrine AR42J. Biochem. Biophys. Res. Commun. *260*, 781–784.

Gaisano, H. Y., Lutz, M. P., Leser, J., Sheu, L., Lynch, G., Tang, L., Tamori, Y., Trimble, W. S., and Salapatek, A. M. (2001). Supramaximal cholecystokinin displaces Munc18c from the pancreatic acinar basal surface, redirecting apical exocytosis to the basal membrane. J. Clin. Invest. *108*, 1597–1611.

Gaisano, H. Y., Sheu, L., Foskett, J. K., and Trimble, W. S. (1994). Tetanus toxin light chain cleaves a vesicle-associated membrane protein (VAMP) isoform 2 in rat pancreatic zymogen granules and inhibits enzyme secretion. J. Biol. Chem. *269*, 17062–17066.

Gaisano, H. Y., Sheu, L., Grondin, G., Ghai, M., Bouquillon, A., Lowe, A., Beaudoin, A., and Trimble, W. S. (1996). The vesicle-associated membrane protein family of proteins in rat pancreatic and parotid acinar cells. Gastroenterology *111*, 1661–1669.

Gaisano, H. Y., Sheu, L., Wong, P. P., Klip, A., and Trimble, W. S. (1997). SNAP-23 is located in the basolateral plasma membrane of rat pancreatic acinar cells. FEBS Lett. *414*, 298–302.

Gallwitz, D., and Jahn, R. (2003). The riddle of the Sec1/Munc-18 proteins–new twists added to their interactions with SNAREs. Trends Biochem. Sci. *28*, 113–116.

Graham, M. E., Barclay, J. W., and Burgoyne, R. D. (2004). Syntaxin/Munc18 interactions in the late events during vesicle fusion and release in exocytosis. J. Biol. Chem. *279*, 32751–32760.

Guo, W., Sacher, M., Barrowman, J., Ferro-Novick, S., and Novick, P. (2000). Protein complexes in transport vesicle targeting. Trends Cell Biol. *10*, 251–255.

Hansen, N. J., Antonin, W., and Edwardson, J. M. (1999). Identification of SNAREs involved in regulated exocytosis in the pancreatic acinar cell. J. Biol. Chem. *274*, 22871–22876.

Honore, B., and Vorum, H. (2000). The CREC family, a novel family of multiple EF-hand, low-affinity Ca(2+)-binding proteins localised to the secretory pathway of mammalian cells. FEBS Lett. *466*, 11–18.

Jahn, R., and Scheller, R. H. (2006). SNAREs–engines for membrane fusion. Nat. Rev. Mol. Cell Biol. *7*, 631–643.

Jahn, R., and Südhof, T. C. (1999). Membrane fusion and exocytosis. Annu. Rev. Biochem. *68*, 863–911.

Johansson, M., Lehto, M., Tanhuanpaa, K., Cover, T. L., and Olkkonen, V. M. (2005). The oxysterol-binding protein homologue ORP1L interacts with Rab7 and alters functional properties of late endocytic compartments. Mol. Biol. Cell *16*, 5480–5492.

Kauppi, M., Jäntti, J., Olkkonen, V. M. (2004). The function of Sec1/Munc18 proteins–solution of the mystery in sight? Top. Curr. Gen. *10*, 115–135.

Kauppi, M., Wohlfahrt, G., and Olkkonen, V. M. (2002). Analysis of the Munc18b-syntaxin binding interface. Use of a mutant Munc18b to dissect the functions of syntaxins 2 and 3. J. Biol. Chem. *277*, 43973–43979.

Kitagawa, M., Williams, J. A., and De Lisle, R. C. (1990). Amylase release from streptolysin O-permeabilized pancreatic acini. Am. J. Physiol. *259*, G157–G164.

Koivu, T., Laitinen, S., Riento, K., and Olkkonen, V. M. (1997). Sequence of a human cDNA encoding Cab45, a Ca2+-binding protein with six EF-hand motifs. DNA Seq. *7*, 217–220.

Laitinen, S., Lehto, M., Lehtonen, S., Hyvärinen, K., Heino, S., Lehtonen, E., Ehnholm, C., Ikonen, E., and Olkkonen, V. M. (2002). ORP2, a homolog of oxysterol binding protein, regulates cellular cholesterol metabolism. J. Lipid Res. *43*, 245–255.

Martin-Verdeaux, S., Pombo, I., Iannascoli, B., Roa, M., Varin-Blank, N., Rivera, J., and Blank, U. (2003). Evidence of a role for Munc18-2 and microtubules in mast cell granule exocytosis. J. Cell Sci. *116*, 325–334.

Misura, K. M., Scheller, R. H., and Weis, W. I. (2000). Three-dimensional structure of the neuronal-Sec1-syntaxin 1a complex. Nature *404*, 355–362.

Nemoto, T., Kimura, R., Ito, K., Tachikawa, A., Miyashita, Y., Iino, M., and Kasai, H. (2001). Sequential-replenishment mechanism of exocytosis in pancreatic acini. Nat. Cell Biol. *3*, 253–258.

Nicoletta, J. A., Ross, J. J., Li, G., Cheng, Q., Schwartz, J., Alexander, E. A., and Schwartz, J. H. (2004). Munc 18-2 regulates the exocytosis of H^+-ATPase in the rat inner medullary collecting duct cell. Am. J. Physiol. *287*, C1366–C1374.

Nielsen, E., Christoforidis, S., Uttenweiler-Joseph, S., Miaczynska, M., Dewitte, F., Wilm, M., Hoflack, B., and Zerial, M. (2000). Rabenosyn-5, a novel Rab5 effector, is complexed with hVPS45 and recruited to endosomes through a FYVE finger domain. J. Cell Biol. *151*, 601–612.

Ohnishi, H., Samuelson, L. C., Yule, D. I., Ernst, S. A., and Williams, J. A. (1997). Overexpression of Rab3D enhances regulated amylase secretion from pancreatic acini of transgenic mice. J. Clin. Invest. *100*, 3044–3052.

Peterson, M. R., Burd, C. G., and Emr, S. D. (1999). Vac1p coordinates Rab and phosphatidylinositol 3-kinase signaling in Vps45p-dependent vesicle docking/fusion at the endosome. Curr. Biol. *9*, 159–162.

Pickett, J. A., and Edwardson, J. M. (2006). Compound exocytosis: mechanisms and functional significance. Traffic *7*, 109–116.

Pinkney, M., Beachey, E., and Kehoe, M. (1989). The thiol-activated toxin streptolysin O does not require a thiol group for cytolytic activity. Infect. Immun. *57*, 2553–2558.

Riento, K., Galli, T., Jansson, S., Ehnholm, C., Lehtonen, E., and Olkkonen, V. M. (1998). Interaction of Munc-18-2 with syntaxin 3 controls the association of apical SNAREs in epithelial cells. J. Cell Sci. *111*, 2681–2688.

Riento, K., Jäntti, J., Jansson, S., Hielm, S., Lehtonen, E., Ehnholm, C., Keränen, S., and Olkkonen, V. M. (1996). A sec1-related vesicle-transport protein that is expressed predominantly in epithelial cells. Eur. J. Biochem. *239*, 638–646.

Riento, K., Kauppi, M., Keränen, S., and Olkkonen, V. M. (2000). Munc18-2, a functional partner of syntaxin 3, controls apical membrane trafficking in epithelial cells. J. Biol. Chem. *275*, 13476–13483.

Rizo, J., and Südhof, T. C. (2002). Snares and Munc18 in synaptic vesicle fusion. Nat. Rev. Neurosci. *3*, 641–653.

Rothman, J. E. (2002). Lasker Basic Medical Research Award. The machinery and principles of vesicle transport in the cell. Nat. Med. *8*, 1059–1062.

Scherer, P. E., Lederkremer, G. Z., Williams, S., Fogliano, M., Baldini, G., and Lodish, H. F. (1996). Cab45, a novel (Ca2+)-binding protein localized to the Golgi lumen. J. Cell Biol. *133*, 257–268.

Tall, G. G., Hama, H., DeWald, D. B., and Horazdovsky, B. F. (1999). The phosphatidylinositol 3-phosphate binding protein Vac1p interacts with a Rab GTPase and a Sec1p homologue to facilitate vesicle-mediated vacuolar protein sorting. Mol. Biol. Cell *10*, 1873–1889.

Toonen, R. F., and Verhage, M. (2003). Vesicle trafficking: pleasure and pain from SM genes. Trends Cell Biol. *13*, 177–186.

Wang, C. C., Ng, C. P., Lu, L., Atlashkin, V., Zhang, W., Seet, L. F., and Hong, W. (2004). A role of VAMP8/Endobrevin in regulated exocytosis of pancreatic acinar cells. Dev. Cell *7*, 359–371.

Wäsle, B., and Edwardson, J. M. (2002). The regulation of exocytosis in the pancreatic acinar cell. Cell Signal. *14*, 191–197.

Whyte, J. R., and Munro, S. (2002). Vesicle tethering complexes in membrane traffic. J. Cell Sci. *115*, 2627–2637.

Williams, J. A. (2006). Regulation of pancreatic acinar cell function. Curr. Opin. Gastroenterol. *22*, 498–504.

Voets, T., Toonen, R. F., Brian, E. C., de Wit, H., Moser, T., Rettig, J., Sudhof, T. C., Neher, E., and Verhage, M. (2001). Munc18-1 promotes large dense-core vesicle docking. Neuron *31*, 581–591.